Available online at www.sciencedirect.com

ScienceDirect

Procedia Structural Integrity 23 (2019) 595–600

Structural Integrity Procedia

www.elsevier.com/locate/procedia

9th International Conference on Materials Structure and Micromechanics of Fracture

Microstructural investigation of defects in photovoltaic cells by the electron beam-induced current method

Nikola Papež[a,*], Rashid Dallaev[a], Dinara Sobola[a,b], Robert Macků[a], Pavel Škarvada[a]

[a] *Department of Physics, Faculty of Electrical Engineering and Communications, Brno University of Technology, Technická 2848/8, Brno, 61600, Czech Republic*
[b] *Central European Institute of Technology, Purkyňova 123, Brno, 61600, Czech Republic*

Abstract

This work aims to clarify the application of electron beam-induced current (EBIC) method for the morphological analysis and detection of local defects and impurities in semiconductor structures such as solar cells. One of the advantages of this method is to observe a leakage path and microplasma sites with nanometer resolution. This technique allows to precisely locate the affected area and determine the type of defect that cannot be commonly characterized with sufficient accuracy. Simultaneously, a focused ion beam could be used to determine junction by milling of the samples at the area of interest. The evaluation results of experimental measurement using these techniques on photovoltaic cells illustrates the applicability and importance of the EBIC method.

Keywords: ebic; structural analysis; solar cells; defects

---

1. Introduction

An important factor affecting the performance of all solar cells is their fabrication quality. The fabrication quality is influenced by various manufacturing processes, material purity or its type. Consequently, the performance and the rate of their degradation may vary depending upon time, temperature, radiation, and other influences. With constant efforts to increase the performance of solar cells, methods for precise locating the defects or imperfections are becoming increasingly important (Kleindiek et al. (2016)). In this work are then studied the influence of defects and imperfections on the function of the solar cell, the influence of

---

[*] Corresponding author.
E-mail address: Nikola.Papez@vutbr.cz

10.1016/j.prostr.2020.01.151

contamination on the pn junction and the overall charge distribution on the structure of the solar cell. Several types of solar cells were also used to compare their differences.

One of the technique for the investigation of electrically active defects and inhomogeneities is electron beam-induced current (EBIC), an analytical method primary for semiconductor characterization (Orlov and Yakimov (2016)). As its name suggests, using the electron beam on a solar cell the induced current of the separated electrons and holes by internal electric field flow through the circuit. If the electric field in the area of the interest is strong, for example within the depletion region of the pn junction, high intensity EBIC signal is produced and correspond with strong image contrast (Xu et al. (2014)).

For the sample to be connected in the circuit, the connection is releasable either directly via the cable when the connectors are out of the sample, otherwise, the sample can be connected to the ohmic contact using so-called nanomanipulators which are very thin probe tips (Arstila et al. (2013)).

2. Materials and methods

All sample manipulating and connecting takes place in the chamber of the scanning electron microscope (SEM) under vacuum condition. The current response is then processed by the picoammeter or current amplifier, A/D converter (ADC) and digital signal processor (DSP) as an image part. The second generation of Tescan's Lyra3 was used as the SEM with standard acceleration voltage up to 30 keV. The voltage was chosen for the highest penetration depth of the electrons in the semiconductor. This increases the probability of finding subsurface defects. Of course, many parameters affect EBIC behavior in addition to the accelerating voltage. This may be, for example, the strength of the contact bonds, the material type or the bias voltage (Papež et al. (2017), Kittler and Seifert (1996)).

Samples measured by the EBIC can be observed in two ways. The first option is to use the *X-EBIC* mode where the electron beam is parallel to the studied junction which is thus in cross-section view (Perez et al. (1998)). This circuit, including the above-mentioned parts, illustrates Fig. 1. The second mode is called *PV-EBIC* where the electron beam is in a plain view from the top in other words perpendicular to the observed surface.

There are plenty of options for what this analytical method can be used. If we measure the semiconductor in X-EBIC mode, we can directly visualize the pn junction. By changing the bias, we can track the different changes in the junction and also measure the I-V characteristic. The typical use for plain view mode is the visualization of grain boundaries, charge distribution and subsurface defects. Electrically inactive and active impurities can also be observed by EBIC.

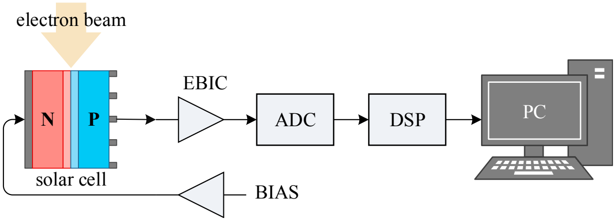

Fig. 1. Electron beam-induced current wiring diagram in X-EBIC mode. The diagram shows an ADC block for analog signal conversion and a DSP block for processing the image part. PV-EBIC mode was also used for investigation of surface and subsurface defects. It differs only in the position of the solar cell.

Specimens of several types of solar cells which differ fundamentally in their structure were used as the studied material to demonstrate their differences in terms of impurities, structural imperfections and defects (Sekiguchi et al. (1996)). Charge distribution was studied on the surface of a polycrystalline Si solar cell, the effect of crack damage on the pn junction was observed in a monocrystalline Si solar cell and the influence of impurities in the layer near the pn junction or contact delamination on a GaAs based solar cell (Ştefan Ţălu et al. (2018), Ştefan Ţălu et al. (2017)).

3. Results

An electrically active impurity was found in the cross-section mode of the GaAs based solar cell in Fig. 4. When increasing the bias, the tunneling occurs and electrons pass through the layer. In the case of the polycrystalline Si cell in Fig. 5 from the top view, an increased charge distribution was also observed under bias operation, especially at the edges of the surface (Smaali et al. (2008)). An electrically inactive region caused by a crack has been discovered on the monocrystalline Si cell in Fig. 6 observed from the cross-section (Marcelot and Magnan (2019)).

For the illustration, figures 2 and 3 showing the GaAs solar cell do not overlap each other as is in the case, for example, for Fig. 5 or Fig. 6, so the difference between SEM and EBIC is apparent. This pair of figures 2 and 3 represents the pn junction and the silver contact of the solar cell. That delamination is already noticeable from Fig. 2, but for Fig. 3 the accurately damaged and delaminated parts are clearly visible. While changing the bias to higher values, the response of the semiconductor becomes less homogeneous and particular structures start to appear. It can be observed that the distribution of carriers close to the contact is different (Yakimov et al. (2009)).

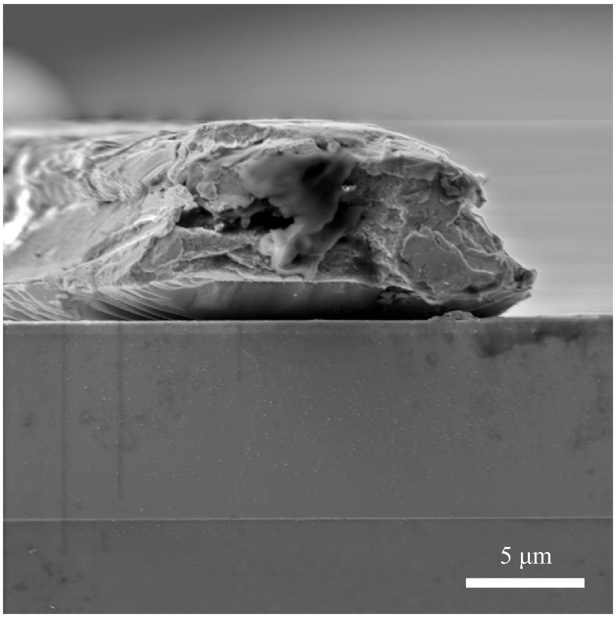

Fig. 2. Image of cross-section of a GaAs solar cell and its contact from SEM without applying the EBIC method.

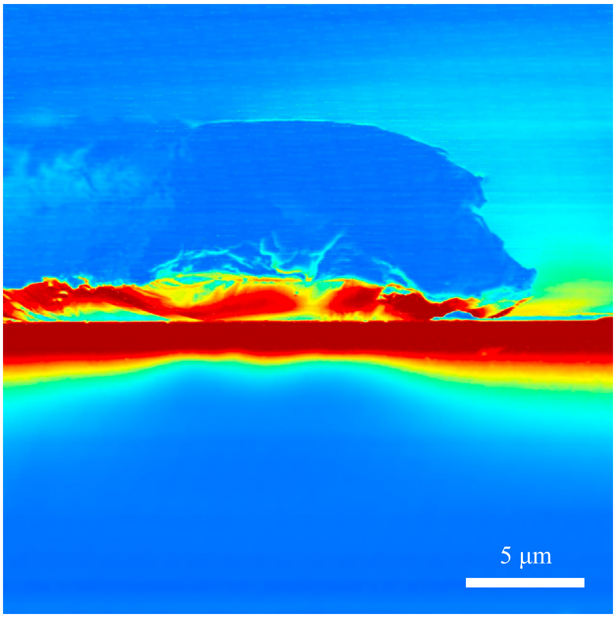

Fig. 3. Applied EBIC method on the solar cell shown in Fig. 2 without SEM image overlay. Area is the same. The exact charge distribution and pn junction can be seen.

The next measurement was performed on a GaAs solar cell where Fig. 4a shows the connected solar cell using nanomanipulators in cross-section mode as described in chapter 1. The electron beam-induced current is not applied to the cell (Fig. 4a–4c) and measurement has proceeded only with a SEM microscope. While observing cell with a larger magnification (Fig. 4b) its top contact is visible which is guided longitudinally relative to the image and it touches the upper nanomanipulator. However, this nanomanipulator is beyond the visible area from Fig. 4b. The full cross-section of the solar cell is now completely visible where is the predominantly germanium serving as the substrate. On the target area where the GaAs layer lies (Fig. 4c), the difference of the carriers can be seen when applying the EBIC method (Fig. 4d). Starting with this image, all other measurements are done using the EBIC method and the images shown by the SEM microscope are slightly overlaid with the colored EBIC picture. Also from Fig. 4d an electrically active impurity is visible in this layer. The origin of these impurities is not clear but most likely, this impurity is fouled during fabrication. During the subsequent increase in the bias from −3 to 1.2 mV which represent Fig. 4d–4i is evident that thanks to this impurity begins to appear tunneling of charge carriers. It is also important to note that this is not a permanent condition and there is no permanent damage after the biasing is reduced (Papež et al. (2018)). As the bias increases further, the potential barrier begins to decrease and due to the influence of impurity it becomes to tunneling from the bias voltage of 1.2 mV. Electrons may then tunnel from one material to the other giving the significant rise to a current.

Silicon solar cells were measured in both X-EBIC and PV-EBIC modes. On the polycrystalline Si from the top view, the charge distribution was measured which is evident in Fig. 5. The noticeable concentration of the charge and leakage path, pointed by an arrow, occurred mainly at the edges of the features on the surface which can negatively affect the performance of the solar cell. Higher created charge density tends to grow with increasing the bias. The behavior of this phenomenon is caused mainly due to imperfections in material production. There are also visible minor impurities (Gajdoš et al. (2018)).

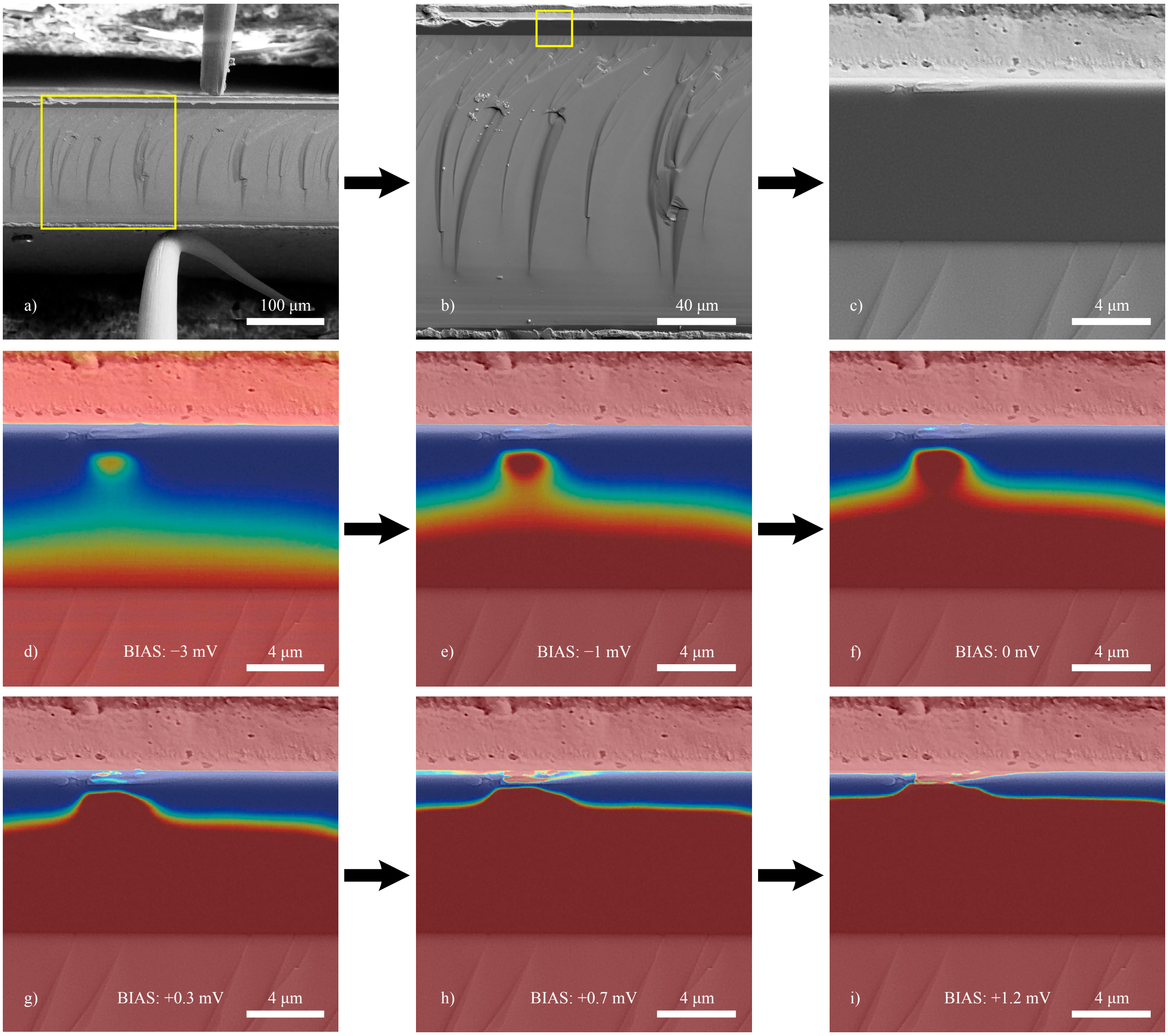

Fig. 4. Electrically active impurity near the junction of GaAs based solar cell in cross-section mode. Images a-c show the subsequent focus on the area of interest, followed by other images d-f where the EBIC method is applied and gradually increased bias from −3 to 1.2 mV.

Another defect can be seen on the monocrystalline Si in the cross-section for which has a typical pyramidal surface composition (Fig. 6). Alongside these pyramidal structures, there is a clearly visible pn junction. In the circle is shown the region, pyramid, which is electrically inactive. This inactive area is caused by a crack located directly below the pyramid structure pointed by an arrow (Papež et al. (2018), Škarvada et al. (2015)).

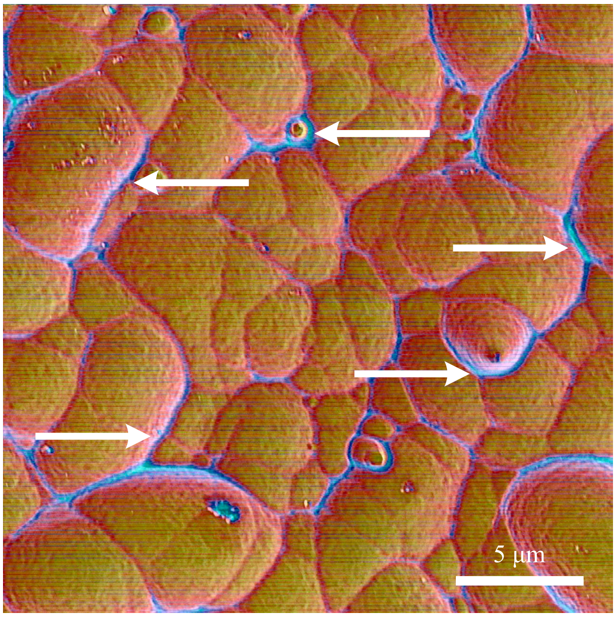

Fig. 5. Charge distribution of the polycrystalline silicon solar cell in PV-EBIC mode from top view. The highest leakages are in the picture presented by blue color and pointed by an arrows.

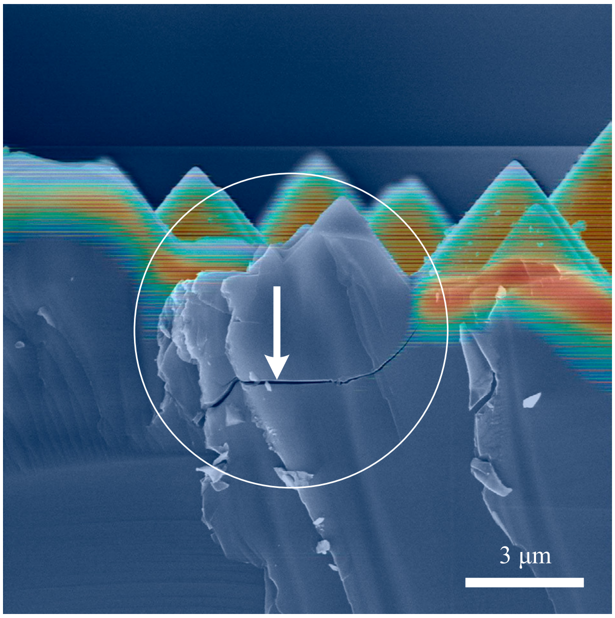

Fig. 6. An electrically inactive part of the monocrystalline silicon solar cell in X-EBIC mode from cross-section view marked with a circle. The crack causing this state is indicated by an arrow.

4. Conclusion

Three types of solar cells were investigated using X-EBIC and PV-EBIC. An electrically active impurity was observed on a GaAs based solar cell which caused electron tunneling. However, it was not a destructive phenomenon and the solar cell was able to get back to its previous condition by reducing bias. Furthermore, a precise view of delamination and its damage of the contact was observed. Also, a different ratio of the charge carriers can be seen near the contact. For the silicon solar cells, charge distribution on their surface and a defect in the pyramidal structure region, which caused it to be electrically inactive, were presented.

Using an EBIC method it has been able to reveal several undesirable defects and impurities which cannot be visible and detectable by SEM and other analytical methods. Many of these defects and impurities are not necessarily caused by improper handling but, for example, by the aging of a solar cell for which is natural to lose its efficiency over time. However, such aging due to various influences can be minimized already during production following strict manufacturing processes. By investigating these results and similar imperfections, it is possible to achieve improved production and prevent, for example, bad fabrication of solar cells.

Acknowledgements

Research described in the paper was financially supported by the Ministry of Education, Youth and Sports of the Czech Republic under the project CEITEC 2020 (LQ1601), by the National Sustainability Program under grant LO1401, and by Internal Grant Agency of Brno University of Technology, Grant No.

FEKT-S-17-4626. For the research, infrastructure of the SIX Center was used. Part of the work was carried out with the support of CEITEC Nano Research Infrastructure (MEYS CR, 2016-2019).

References

Arstila, K., Hantschel, T., Schulze, A., Vandooren, A., Verhulst, A., Rooyackers, R., Eyben, P., Vandervorst, W., 2013. Nanoprober-based ebic measurements for nanowire transistor structures. Microelectronic Engineering 105, 99 – 102. URL: http://www.sciencedirect.com/science/article/pii/S016793171200439X, doi:https://doi.org/10.1016/j.mee.2012.08.006.

Gajdoš, A., Škarvada, P., Macků, R., Papež, N., Ľubomír Škvarenina, Sobola, D., 2018. Isolation and optoelectronic characterization of si solar cells microstructure defects 1124, 1–6. doi:10.1088/1742-6596/1124/4/041009.

Škarvada, P., Ľubomír Škvarenina, Sobola, D., Macků, R., Tománek, P., Grmela, L., 2015. Multiscale characterization of solar cells, in: Progress in Applied Surface, Interface and Thin-film Science 2015, Comenius University, Comenius University. pp. 148–151.

Kittler, M., Seifert, W., 1996. Ebic defect characterisation: state of understanding and problems of interpretation. Materials Science and Engineering: B 42, 8 – 13. URL: http://www.sciencedirect.com/science/article/pii/S0921510796016777, doi:https://doi.org/10.1016/S0921-5107(96)01677-7. 4th International Workshop on Beam Injection Assessment of Defects in Semiconductors.

Kleindiek, S., Schock, K., Rummel, A., Zschornack, M., Limbecker, P., Meyer, A., Kemmler, M., 2016. Current imaging, ebic/ebac, and electrical probing combined for fast and reliable in situ electrical fault isolation. Microelectronics Reliability 64, 313 – 316. URL: http://www.sciencedirect.com/science/article/pii/S0026271416301688, doi:https://doi.org/10.1016/j.microrel.2016.07.024. proceedings of the 27th European Symposium on Reliability of Electron Devices, Failure Physics and Analysis.

Ştefan Ţălu, Papež, N., Sobola, D., Achour, A., Solaymani, S., 2017. Micromorphology investigation of gaas solar cells: case study on statistical surface roughness parameters 28, 1–12. doi:10.1007/s10854-017-7422-4.

Ştefan Ţălu, Papež, N., Sobola, D., Tofel, P., 2018. Fractal analysis of the 3-d surface topography of gaas solar cells, in: DEStech Transactions on Environment, Energy and Earth Sciences, DEStech Publications, Inc., DEStech Publications, Inc.. pp. 489–493.

Marcelot, O., Magnan, P., 2019. From ebic images to qualitative minority carrier diffusion length maps. Ultramicroscopy 197, 23 – 27. URL: http://www.sciencedirect.com/science/article/pii/S0304399118302225, doi:https://doi.org/10.1016/j.ultramic.2018.11.005.

Orlov, V., Yakimov, E., 2016. Extended defect study in si: Ebic versus lbic. Superlattices and Microstructures 99, 202 – 207. URL: http://www.sciencedirect.com/science/article/pii/S0749603616300830, doi:https://doi.org/10.1016/j.spmi.2016.02.040. 16th international conference on Defects, Recognition, Imaging and Physics in Semiconductors.

Papež, N., Ľubomír Škvarenina, Tofel, P., Sobola, D., 2017. Thermal stability of gallium arsenide solar cells, in: Photonics, Devices, and Systems VII, pp. 543–548.

Papež, N., Sobola, D., Gajdoš, A., Ľubomír Škvarenina, Macků, R., Eliáš, M., Nebojsa, A., Motúz, R., 2018. Surface morphology after reactive ion etching of silicon and gallium arsenide based solar cells 1124, 165–171. doi:10.1088/1742-6596/1124/4/041015.

Papež, N., Sobola, D., Ľubomír Škvarenina, Škarvada, P., Hemzal, D., Tofel, P., Grmela, L., 2018. Degradation analysis of gaas solar cells at thermal stress. Applied Surface Science 461, 212 – 220. URL: http://www.sciencedirect.com/science/article/pii/S016943321831393X, doi:https://doi.org/10.1016/j.apsusc.2018.05.093. 5th Progress in Applied Surface, Interface and Thin Film Science and Solar Renewable Energy News.

Perez, G., Courtade, F., Benteo, B., Gauffier, J.L., Kwang, J., 1998. Junction delineation and ebic on fib cross section. Microelectronics Reliability 38, 907 – 912. URL: http://www.sciencedirect.com/science/article/pii/S0026271498001048, doi:https://doi.org/10.1016/S0026-2714(98)00104-8. reliability of Electron Devices, Failure Physics and Analysis.

Sekiguchi, T., Shen, B., Watanabe, T., Sumino, K., 1996. Ebic study on the electrical activity of stacking faults in silicon. Materials Science and Engineering: B 42, 235 – 239. URL: http://www.sciencedirect.com/science/article/pii/S0921510796017138, doi:https://doi.org/10.1016/S0921-5107(96)01713-8. 4th International Workshop on Beam Injection Assessment of Defects in Semiconductors.

Smaali, K., Fauré, J., Hdiy, A.E., Troyon, M., 2008. High-resolution scanning near-field ebic microscopy: Application to the characterisation of a shallow ion implanted p+–n silicon junction. Ultramicroscopy 108, 605 – 612. URL: http://www.sciencedirect.com/science/article/pii/S0304399107002276, doi:https://doi.org/10.1016/j.ultramic.2007.10.009.

Xu, L., Hameiri, Z., Weber, K., Yang, X., 2014. Comparison between secondary electron microscopy dopant contrast image (semdci) and electron beam induced current (ebic) for laser doping of crystalline silicon. Energy Procedia 55, 179 – 185. URL: http://www.sciencedirect.com/science/article/pii/S187661021401337X, doi:https://doi.org/10.1016/j.egypro.2014.08.112. proceedings of the 4th International Conference on Crystalline Silicon Photovoltaics (SiliconPV 2014).

Yakimov, E., Vergeles, P., Govorkov, A., Polyakov, A., Smirnov, N., Lee, I.H., Lee, C.R., Pearton, S., 2009. Ebic investigations of defect distribution in elog gan films. Physica B: Condensed Matter 404, 4916 – 4918. URL: http://www.sciencedirect.com/science/article/pii/S0921452609009673, doi:https://doi.org/10.1016/j.physb.2009.08.215.